With the development of simulation technology and the ability to obtain accurate numerical results, as well as with the development of information technology, software that can solve numerical problems has become necessary to see physical changes that cannot be seen by the human eye. Multiphase stream field is settled utilizing the volume of fluid (VOF) method, and the flow equations are assessed and addressed mathematically by the notable limited volume approach. As a multiphase framework without mass exchange, air/water stream is considered. For practically all cases considered in this review, the heat transfer coefficient is higher. In any case, a critical punishment pressure drop was observed especially for high mass courses through undulating channels. A wavy channel with a variable wave height was simulated to see the variables of the flow process for multi-phase materials with a square cross-section, where different speeds were used for the inlet duct for air, water and steam. The results proved that the increase in the height of the channel wall wave works to obstruct the flow and thus increases the time required for the fluid to reach the exit area. The value of time required for steam and air to reach the exit area at the channel wall wave height of 25 mm and the flow velocity of 0.1 m/s was 6.01 s, which is the longest time it took for the fluid to reach the exit area compared to other cases. The pressure value reflects the amount of turbulence in the flow process, and it's crucial for thermal improvements based on flow turbulence. The entrance flow velocity is 0.1 m/s and the wall wave height is 25 mm at a time of 2 s, when the pressure reaches 873.7 Pa

Keywords: numerical simulation, multiphase flow, rippled channel, CFD, sinusoidal duct

UDC 621
DOI: 10.15587/1729-4061.2022.263587

IDENTIFYING THE EFFECT OF CHANNEL WALL RIPPLE HEIGHT ON MULTIPHASE FLOW

Mohammed Ali Mahmood Hussein
Corresponding author
Doctor of Engineering, Assistant Professor*
E-mail: Mohamed.ali71@ruc.edu.iq
Wajeeh Kamal Hasan
Doctor of Mechanical Engineering,
Assistant Professor*
*Department of Refrigeration
and Air Conditioning Engineering
Al-Rafidain University College
Palestine ST str., 10, Baghdad, Iraq, 10001

Received date 17.06.2022
Accepted date 23.08.2022
Published date 30.08.2022

How to Cite: *Hussein, M. A. M., Hasan, W. K. (2022). Identifying the effect of channel wall ripple height on multiphase flow. Eastern-European Journal of Enterprise Technologies, 4 (7 (118)), 51–60. doi: https://doi.org/10.15587/1729-4061.2022.263587*

1. Introduction

Software that can solve numerical problems is now essential to seeing physical changes that are invisible to the human eye, thanks to advances in simulation technology, the ability to produce correct numerical results, and the proliferation of advances in information technology. The volume of fluid (VOF) method is used to solve the multiphase flow field, and the flow equations are quantitatively evaluated and solved using the prominent constrained volume approach. With a relatively low-pressure drop penalty, sinusoidal wavy channels have consistently outperformed straight channels in terms of thermal performance. As a result, wavy channels can be employed to cool gas turbine blades and even tiny heat exchangers. The creation of secondary flows (in the form of 3D vortices) inside the troughs of the corrugated channel is responsible for the desirable thermo-hydraulic performance of wavy channels. For engineering applications, two-phase flow characteristics in ducts and tubes that are not straight are more complicated and crucial. These kinds of complex geometries have been used in some numerical studies on flow characteristics. Compact heat exchangers and high-efficiency membrane oxygenators are two examples of practical applications that involve fluid mixing and complex geometry, such as wavy walled channels. Therefore, studies devoted to simulating the flow process in an undulating duct of variable wave height are of scientific relevance.

2. Literature review and problem statement

A wavy channel with a variable wave height was simulated to see the variables of the flow process for multi-phase materials. Different speeds were used for the inlet duct for air, water and steam. The models for extracting stage speeds were then settled [1]. This work presents a creative strategy to thoroughly reveal the stream insecurity of a three-stage oil-gas-water stream. A multi-channel conductance sensor is used to capture definite stream structure data at various points along the line cross area in a 20 mm internal width pipe [2]. In an upward wavy channel, tumultuous gas-fluid multiphase streams with and without work change are cared to. Inside wavy channels, condensing streams of refrigerant R134a are imitated. Inventor Timperio's theory of fluid mechanics has shown that in almost all circumstances, the convective heat transfer coefficient in wavy guides is larger than in straight channels [3]. For heavy mass motions through wavy channels, a massive strain drop discipline is seen [4]. A trial and mathematical recreation was created to investigate the slug stream connection with a flat line get together under different shallow gas and fluid speeds [5]. Recent progress in computing power has led to a great advance in computational fluid dynamics (CFD) and computational structural dynamics (CSD) [6]; so, many researchers are trying to solve problems by coupling the equation of motion for the fluid with that for the structure. The interaction of fine particles with an expanding gas flow

under fluidization conditions is considered. The objects of study are finely dispersed materials, their single particles, gas flow in a fluidized layer [7].

Investigations made by other researchers [8] show the enhanced heat transfer system connected to ultrasonic vibration. They discussed the sinusoidal ultrasonic transmission techniques. An ultrasonic impact might be attributed to three factors, all of which are caused by the building cycle in an ultrasonic cavitation system. There are two significant stream designs related to even and strayed wells. Attributable to the variable stream rate, water content, and pipeline tendency, change qualities for the progress from delineated to annular or scattered streams are not satisfactory. A forecast model for the twisting of the interfacial wave was developed [9]. Other researchers [10] proposed a novel on-line, contactless and almost non-meddling estimation technique for gas-fluid slug streams. Temperature vacillations of a line divider warmed at a consistent heat transfer are actuated by Taylor air pockets and fluid slugs, a cavitation-based soft abrasive flow (CSAF) handling strategy to deal with apparatus created by [11]. Based on the results of a numerical study into the stress-strain state of the dent zone in the tank wall [12], a mathematical model was chosen to find the stress-strain state of the wall of a cylindrical tank with variable thickness, which proved the assumption of significant stress concentrations in the dent zone and indicated the determining effect on the concentration of stresses in the dent zone exerted by its geometric dimensions and its depth in particular.

Most of the previous research had difficulties in managing program settings because it was difficult to apply it to normal computers because it required rather powerful computers to solve the equations when increasing the number of fluid phases. Therefore, researchers focused on how to simulate two different phases of matter and study phase patterns in a straight channel. All this allows us to assert that it is expedient to conduct a study on simulating multi-phase flow patterns in a wave channel.

3. The aim and objectives of the study

The aim of the study is to simulate phase flow patterns in a rippled wall channel.

To achieve the aim, the following objectives are accomplished:

– to investigate the effect of using different velocities on the flow;

– to examine different wave heights;

– to study the multi-phase flow in an undulating channel;

– to study the effect of velocity and wall wave height on the time it takes the fluid to reach the exit area.

4. Materials and methods

4. 1. Object and hypothesis of the study

The volume of fluid (VOF) method is utilized to resolve the multiphase flow field, and the well-known limited volume method is used to analyze and solve the equations in an objective manner. The air/water stream is thought of as a multiphase framework because there is no mass exchange taking place in it.

Researchers were able to determine the factors that affect the flow process for multi-phase materials with a square cross-section by modifying the intake duct's velocities for the air, water, and steam. This research uses a multiphase flow to examine the ripple on a channel wall and the resultant impact.

In the current study, water, air, and vapor are considered as the running liquid and the flow characteristics are assumed to be:

– transient;
– two-dimensional;
– Newtonian;
– incompressible;
– turbulent.

The work was done in a two-dimensional form to reduce the high mesh numbers, ease the solution and reduce the run time.

4. 2. Model development

The simulation process of the optimization model requires an engineering program to design. The model was designed using the SolidWorks program with the channel dimensions of 1,200 mm in length and 100 mm in height, the channel contains three bends with a variable wave height ranging from 5 mm to 25 mm and a wavelength of 50 mm as in Fig. 1.

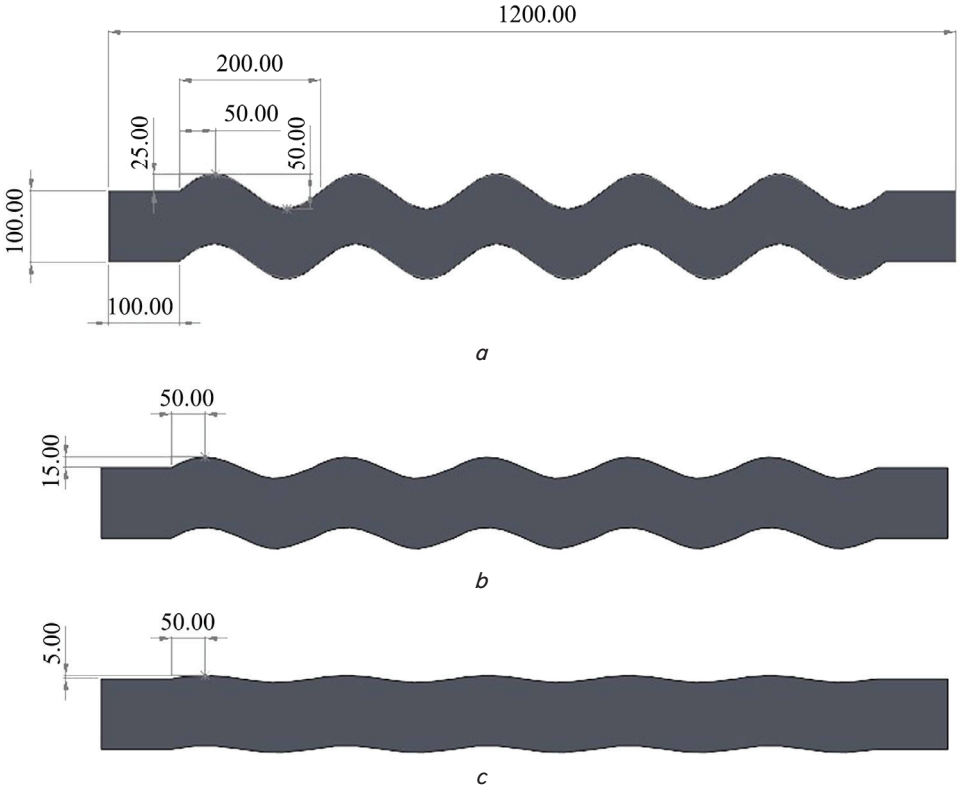

Fig. 1. Geometry dimensions with different ripple heights: *a* – 25 mm; *b* – 15 mm; *c* – 5 mm

After the process of designing the model and starting the simulation using CFD software, an engineering program simulates fluid flow, where a suitable mesh must be made for obtaining accurate results that can be compared to practical applications. The mesh reliability and mesh increase until a stable result is reached, Table 1, Fig. 2. A tetrahedral grid was used with a number of elements that reached 120,725, the pressure in this case was stable and its value was 108.6 Pa.

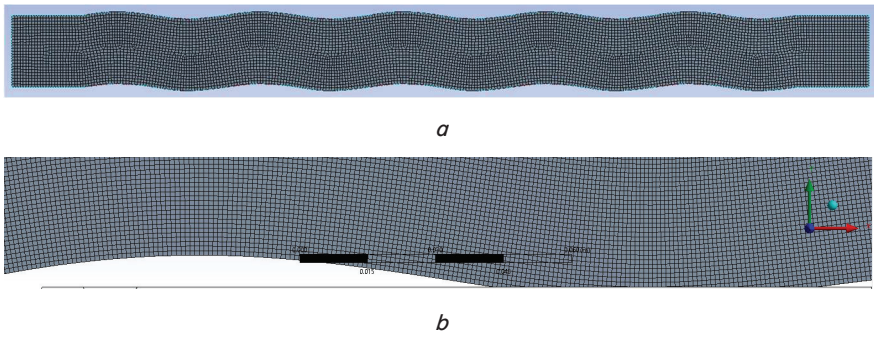

a

b

Fig. 2. Mesh geometry: *a* – the entire geometry; *b* – closer look at the mesh

Table 1

Mesh independency

Case	Element	Node	Pressure (Pa)
1	56,342	60,724	112.4
2	73,875	85,628	109.9
3	99,635	100,625	108.7
4	119,494	120,725	108.6

After the process of completing the mesh reliability, the case settings were entered using the CFD processor for fluid and thermal simulation. Three phases were used, which represent water, air and water vapor, where water is the main phase in these simulations. These fluids enter with the same entry speed and variable in cases, which are 0.1, 0.5, 1 m/s. The wall wave has different values of 5 mm, 15 mm, 25 mm to see changes in the state of the fluids and compare them with each other.

4. 3. Governing equations

4. 3. 1. Volume Fraction Equation

The solution of a continuity equation for the volume fraction of one (or more) of the phases is used to trace the interface (s) between the phases. This equation has the following form for the *q*-th phase:

$$\frac{1}{\rho_q}\left[\begin{array}{l}\frac{\partial}{\partial t}\left(\alpha_q\rho_q\right)+\nabla\cdot\left(\alpha_q\rho_q\vec{v}_q\right)= \\ =S_{\alpha_q}+\sum_{p=1}^{n}\left(\dot{m}_{pq}-\dot{m}_{qp}\right)\end{array}\right], \quad (1)$$

where $\dot{m}_{qp}$ represents mass transfer from phase *q* to phase *p*, and $\dot{m}_{pq}$ represents mass transfer from phase *p* to phase *q*. The right-hand side source term, S_{α_q}, is zero by default, but you can provide a constant or user-defined mass source for each phase. For additional information on mass transfer modeling in Ansys Fluent's generic multiphase models, see Modeling Mass Transfer in Multiphase Flows.

For the primary phase, the volume fraction equation will not be solved; instead, the primary-phase volume fraction will be determined using the following constraint:

$$\sum_{q=1}^{n}\alpha_q=1. \quad (2)$$

The volume fraction equation can be solved either through implicit or explicit time formulation.

4. 3. 2. Implicit Formulation

The volume fraction equation is discretized in the following way when the implicit formulation is used:

$$\frac{\alpha_q^{n+1}\rho_q^{n+1}-\alpha_q^n\rho_q^n}{\Delta t}V+ \\ +\sum_f\left(\rho_q^{n+1}U_f^{n+1}\alpha_{q,f}^{n+1}\right)= \\ =\left[S_{\alpha_q}+\sum_{p=1}^{n}\left(\dot{m}_{pq}-\dot{m}_{qp}\right)\right]V, \quad (3)$$

where n+1 – index for current time step; n – index for previous time step; α_q^{n+1} – cell value of volume fraction at time step n+1; α_q^n – cell value of volume fraction at time step n; $\alpha_{q,f}^{n+1}$ – face value of the q^{th} volume fraction at time step n+1; U_f^{n+1} – volume flux through the face at time step n+1; V – cell volume. A scalar transport equation is solved iteratively for each of the secondary-phase volume fractions at each time step since the volume fraction at the current time step is a function of other values at the current time step.

The selected spatial discretization technique is used to interpolate face fluxes. In the User's Guide, Spatial Discretization Schemes for Volume Fraction, the schemes available in Ansys Fluent for the implicit formulation are discussed.

Both time-dependent and steady-state computations can be done using the implicit approach. For further information, see Choosing Volume Fraction Formulation in the User's Guide.

4. 3. 3. Material Properties

The existence of component phases in each control volume determines the attributes that appear in the transport equations. If the phases are denoted by the subscripts 1 and 2, and the volume fraction of the second of these is monitored in a two-phase system, the density in each cell is given by

$$\rho=\alpha_2\rho_2+\left(1-\alpha_2\right)\rho_1. \quad (4)$$

In general, for an *n*-phase system, the volume-fraction-averaged density takes on the following form:

$$\rho=\Sigma\,\alpha_q\rho_q. \quad (5)$$

All other properties (for example, viscosity) are computed in this manner.

4. 3. 4. Momentum Equation

The velocity field is shared throughout the phases after a single momentum equation is solved over the domain.

The volume fractions of all phases are dependent on the momentum equation, as illustrated below, through the characteristics.

$$\frac{\partial}{\partial t}(\rho\vec{v})+\nabla\cdot(\rho\vec{v}\vec{v})=-\nabla p+$$
$$+\nabla\cdot\left[\mu\left(\nabla\vec{v}+\nabla\vec{v}^{T}\right)\right]+\rho\vec{g}+\vec{F}. \quad (6)$$

One drawback of the shared-fields approach is that in circumstances when the phases have considerable velocity differences, the accuracy of the velocities estimated near the interface might suffer.

It's worth noting that if the viscosity ratio is more than 1×10^3, it might cause problems with convergence. The compressive interface capturing scheme for arbitrary meshes (CICSAM) solves the problem of poor convergence by being suited for flows with large ratios of viscosities between the phases.

4. 3. 5. Energy Equation

The energy equation, also shared among the phases, is shown below.

$$\frac{\partial}{\partial t}(\rho E)+\nabla\cdot\left(\vec{v}(\rho E+p)\right)=$$
$$=\nabla\cdot\left(\begin{array}{l}k_{eff}\nabla T-\sum_{q}\sum_{j}h_{j,i}\vec{J}_{j,q}+\\+\left(\bar{\tau}_{eff}\cdot\vec{v}\right)\end{array}\right)+S_h, \quad (7)$$

where k_{eff} is the effective conductivity, $\vec{J}$ is the diffusion flow of species j, $h_{j,i}$ is enthalpy, $\vec{J}_{j,q}$ is the diffusive flow of species j in phase q, according to the Volume of Fluid (VOF) Model Theory. Energy transfer due to conduction, species diffusion, and viscous dissipation are the first three terms on the right-hand side, respectively. Because species formation enthalpy is already included in the overall enthalpy calculation as detailed in Energy Sources Due to Reaction, S_h includes volumetric heat sources that you have established but excludes heat sources created by finite-rate volumetric or surface reactions. The VOF model treats energy, E, as a mass-averaged variable:

$$E=\frac{\sum_{q=1}^{n}\alpha_q\rho_q E_q}{\sum_{q=1}^{n}\alpha_q\rho_q}, \quad (8)$$

$$E_q=h_q-\frac{p}{\rho_q}+\frac{v^2}{2}, \quad (9)$$

where h_q for each phase is based on the specific heat of that phase and the shared temperature. The properties ρ, k_{eff} (effective thermal conductivity) and μ_{eff} (effective viscosity) are calculated by volumetric averaging over the phases. The source term, S_h, contains contributions from radiation, as well as any other volumetric heat sources.

5. Results of using different velocities and an undulating channel

5. 1. Effect of fluid ingress velocity on steam flow turbulence

Through these results, and by changing the entry velocity of the three fluids used, we can observe the effect of the velocity of the inlet flow on the time taken for steam to reach the exit area. Fig. 3 shows changes in the shape of the flow with time, where the height of the wall wave affects the shape of the flow of steam or air alike. Note that at a velocity of 0.1 m/s for all fluids, the time taken for the flow to reach the exit area was 3.01 s at the wave height of 5 mm as the flow takes the form of a slug inside the channel even with a change in the location of the flow.

As for Fig. 4, the velocity of the flow increased to 0.5 m/s at the wall wave height of 5 mm, where it is noted that the time taken for the flow to reach the exit area decreased and reached 1.57 s. As for the wave shape, it took the shape of a slug over time.

In Fig. 5, the velocity of flow entry for the three fluids is 1 m/s while the wall wave height remains 5 mm.

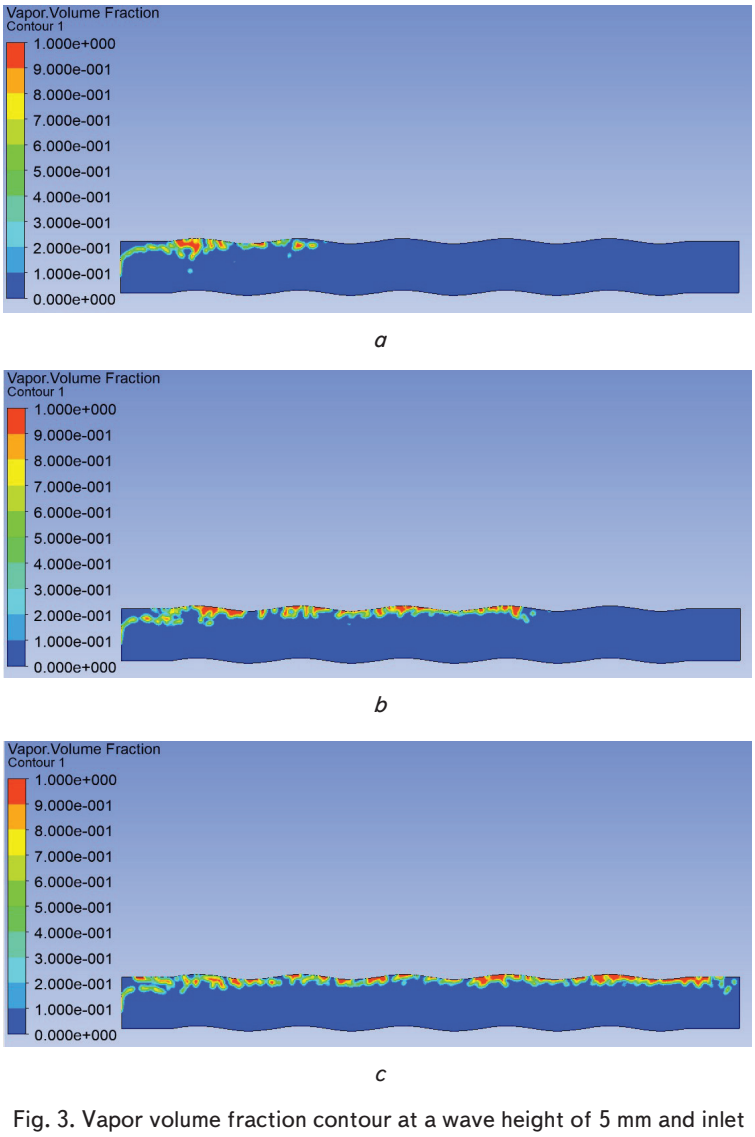

Fig. 3. Vapor volume fraction contour at a wave height of 5 mm and inlet velocity of 0.1 m/s: *a* – 1 s; *b* – 2 s; *c* – 3.01

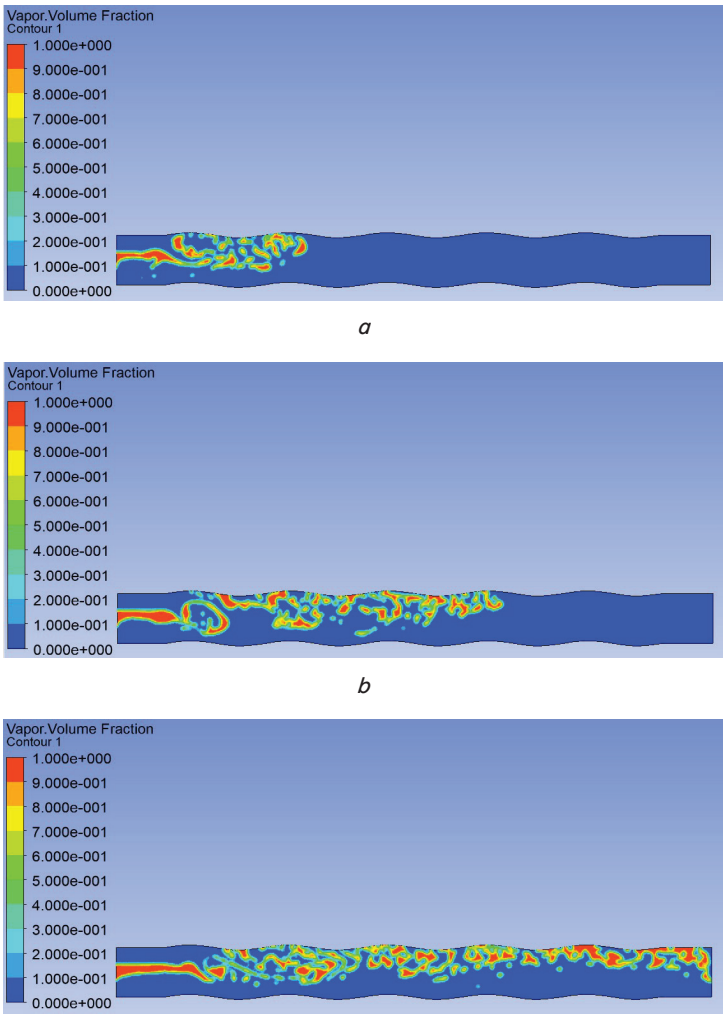

Fig. 4. Vapor volume fraction contour at a wave height of 5 mm and inlet velocity of 0.5 m/s: *a* – 0.5 s; *b* – 1 s; *c* – 1.57 s

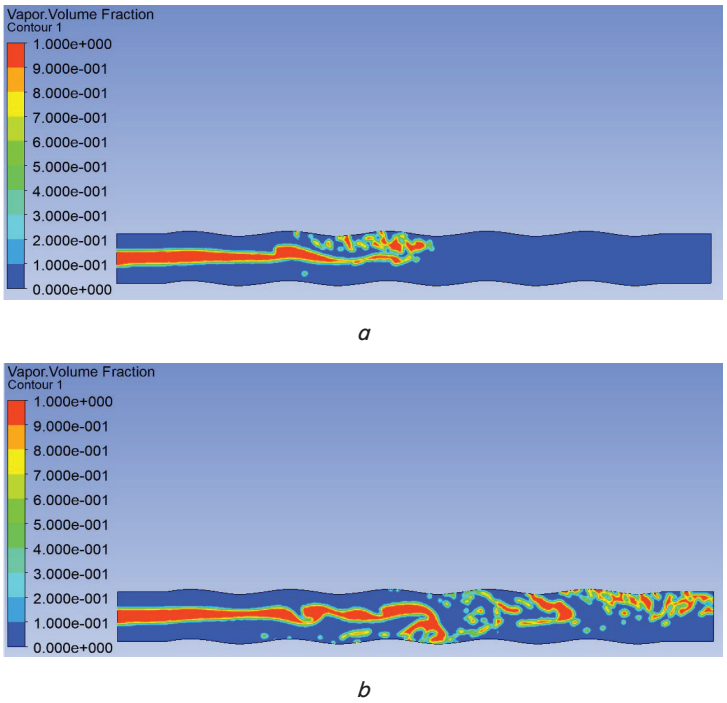

Fig. 5. Vapor volume fraction contour at a wave height of 5 mm and inlet velocity of 1 m/s: *a* – 0.5 s; *b* – 0.97 s

It is noted that the time taken for the flow to reach the exit area is 0.97 s, which is the lowest value of time compared to the rest of the cases, where it is noted that the shape of the flow changed and shifted from slug to annular.

5. 2. Effect of wall wave height on steam turbulence

The height of the wall wave greatly affects the flow of the incoming fluids and disturbs the flow and thus increases the time it takes for the flow to reach the exit area. Fig. 6 represents the fluid inlet flow velocity of 0.1 m/s and the wave wall height of 15 mm. The turbulence value increased significantly at a wall wave height of 5 mm. It took 4.48 s for the fluid flow to reach the exit area where it took the shape of slug flow. However, in Fig. 7, the value of the wall wave height became 25 mm, thus increasing the turbulence of the wave.

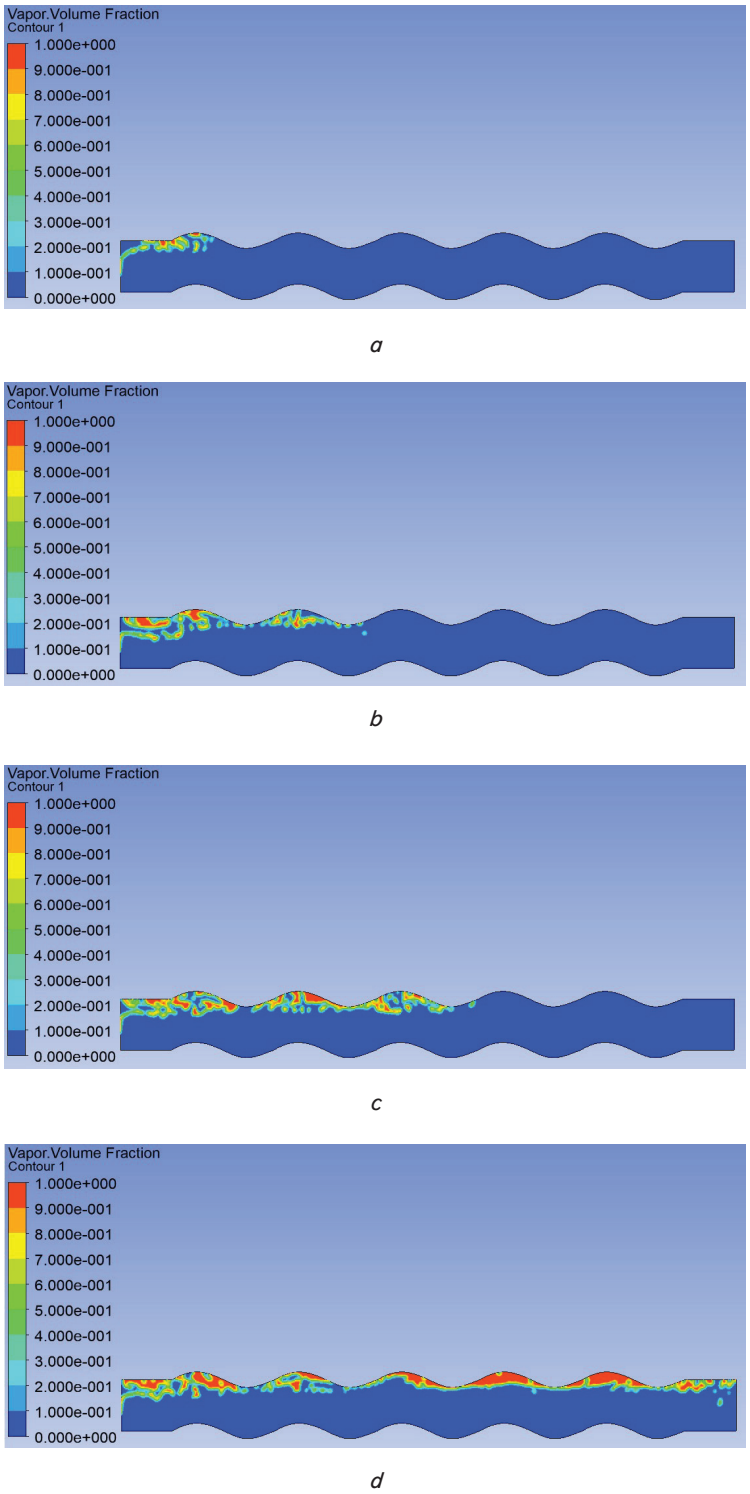

Fig. 6. Vapor volume fraction contour at a wave height of 15 mm and inlet velocity of 0.1 m/s: *a* – 0.5 s; *b* – 1.5 s; *c* – 2.5 s; *d* – 4.48 s

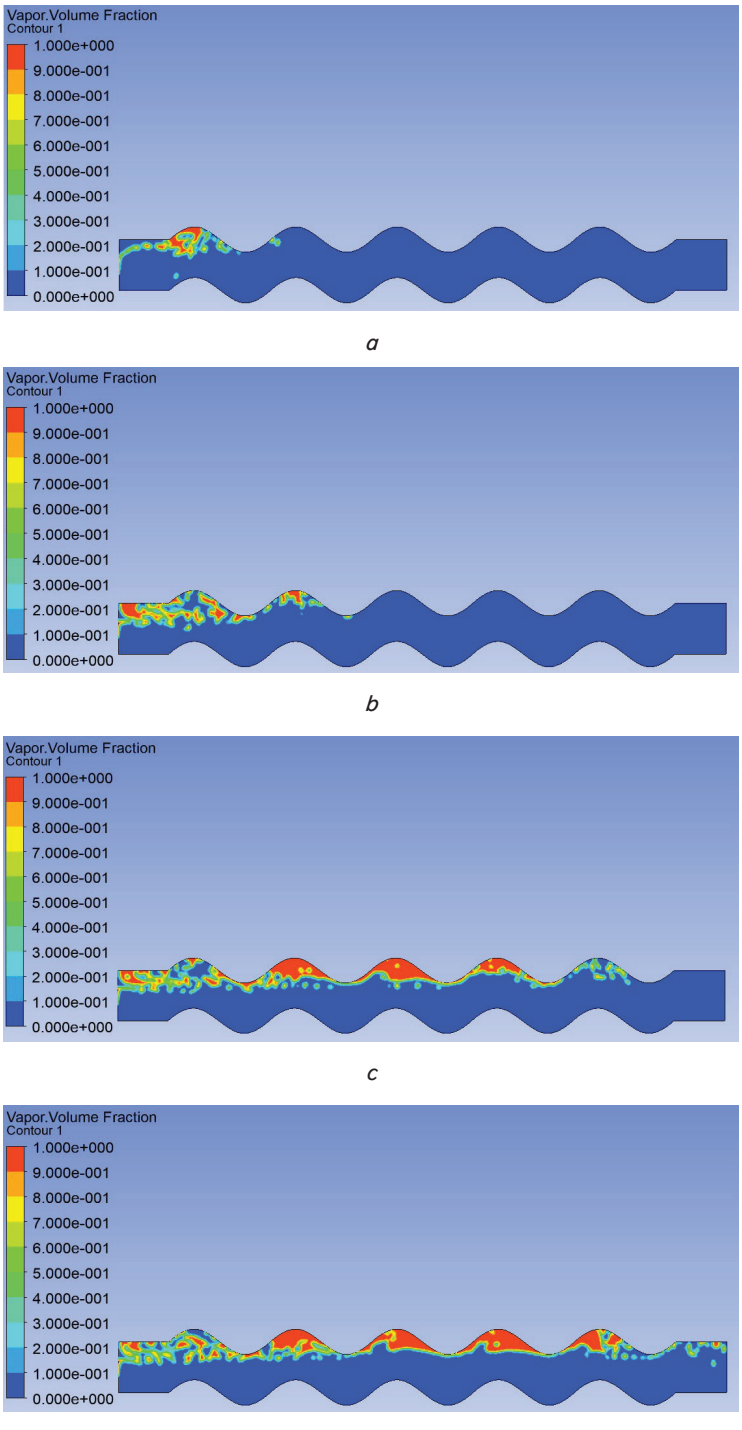

Fig. 7. Vapor volume fraction contour at a wave height of 25 mm and inlet velocity of 0.1 m/s: *a* – 1 s; *b* – 2 s; *c* – 5 s; *d* – 6.01 s

Certainly, the time taken for the flow to reach the exit area increased, where its value was 6.01 m/s, which is the time taken for the flow to reach the exit area where the flow took the shape of a slug.

5. 3. Effect of variable fluids on pressure value

One of the most important variables that can be calculated by using more than one phase of the flow is the pressure. The pressure value indicates the amount of turbulence in the flow process. In addition, it is important in thermal improvements based on the turbulence of the flow, as it is noted in Fig. 8 that the pressure value gradually increased until reaching the time of 2 s, where the pressure reached 873.7 Pa, in the case, the inlet flow velocity is 0.1 m/s and the wall wave height is 25 mm.

After the time of 2 s, the pressure value starts descending until the flow reaches the exit area at the time of 6.01 s, where the pressure value was 213.9 Pa and the reason for this is the stability of the flow and the homogeneity of the fluid phases with each other.

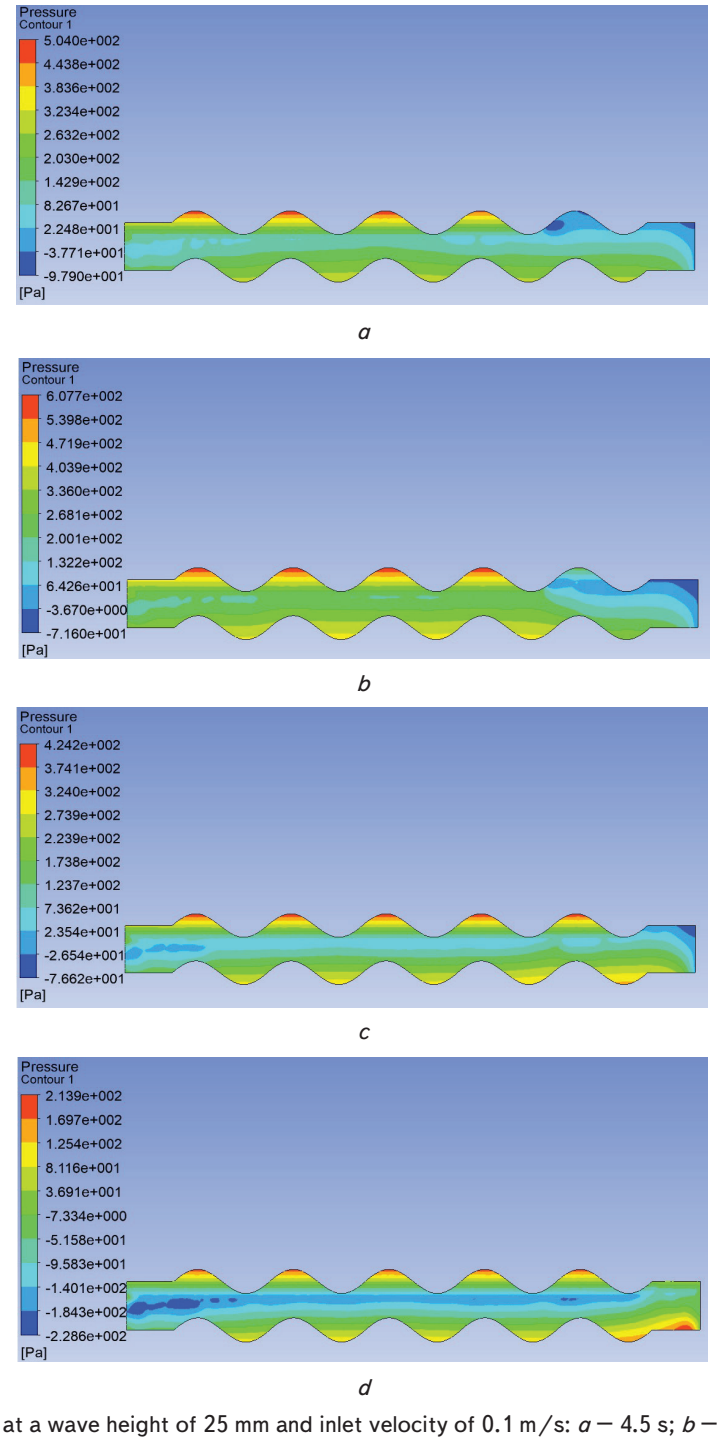

Fig. 8. Pressure contour at a wave height of 25 mm and inlet velocity of 0.1 m/s: *a* – 4.5 s; *b* – 5 s; *c* – 5.5 s; *d* – 6.01 s

5. 4. Effect of velocity and wall wave height on the time it takes for the fluid to reach the exit area

Fig. 9 shows the cases that were taken with changes in the height of the wall wave and the amplitude of the flow entering the three phases.

It is noted that the value of the time taken for the flow to reach the exit area is directly proportional to the height of the wall wave and inversely to the speed of the entry flow of the three phases.

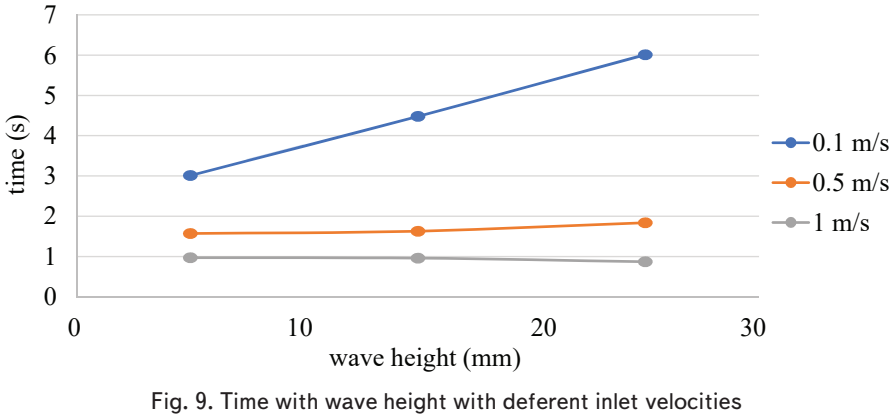

Fig. 9. Time with wave height with deferent inlet velocities

6. Discussion of the results of using different velocities and an undulating channel

It is noted that the time taken for the flow to reach the exit area is 0.97 s, which is the lowest value of time compared to the rest of the cases, where it is noted that the shape of the flow changed and shifted from slug to annular. The reason for this is the velocity of fluid flow through a semi-planar channel. It was also found that the height of the wall wave greatly affects the flow of the incoming fluids and disturbs the flow and thus increases the time it takes for the flow to reach the exit area. It is noted in Fig. 8 that the pressure value gradually increased until reaching the time of 2 s, where the pressure reached 873.7 Pa, in the case, the inlet flow velocity is 0.1 m/s and the wall wave height is 25 mm. The reason for this is that the entry area comes after a flat area and then enters the ripple area in the channel.

The advantage of this study is the simulation of multiple fluids in one channel and identification of the two bells of these fluids together to see the difference in velocities and densities between them and the turbulence that occurs.

The limits that were encountered in the simulation study are that it is not possible to create more than 3 fluids together to obtain correct results that match the truth.

The study was limited to the extent of the influence of multiple fluids, and its usefulness on heat energy transfer and benefiting from the turbulence in multiple fluids was not addressed.

This study can be carried out in the future experimentally and the results obtained can be compared with the numerical results.

7. Conclusions

1. The velocity of the flow increased to 0.5 m/s at the height of the wall wave of 5 mm. It is noted that the time taken for the flow to reach the exit area decreased and reached 1.57 s. As for the wave shape, it took the shape of a slug over time. The velocity of flow entry for the three fluids is 1 m/s while the wall wave height remains 5 mm. It is noted that the time taken for the flow to reach the exit area is 0.97 s, which is the lowest value of time compared to the rest of the cases, where the shape of the flow changed and shifted from slug to annular.

2. The height of the wall wave greatly affects the flow of the incoming fluids, disturbs the flow, and thus increases the time it takes for the flow to reach the exit area. At the fluid inlet flow velocity of 0.1 m/s and the wave wall height of 15 mm, the turbulence value increased significantly from 5 mm to 25 mm.

3. The pressure value indicates the amount of turbulence in the flow process, and it is important in thermal improvements based on the turbulence of the flow. The pressure value gradually increases until reaching the time of 2 s, where the pressure reached 873.7 Pa, in the case, the inlet flow velocity is 0.1 m/s and the wall wave height is 25 mm.

4. The value of the time taken for the flow to reach the exit area is directly proportional to the height of the wall wave and inversely to the speed of the entry flow of the three phases. The cases were reviewed taken with changes in the height as well as the amplitude of the flow entering and exiting the three stages. The time taken for steam to reach the exit area at a height of 5 mm, where the flow takes the form of a slug inside the channel even with a change in the location of the flow. At a velocity of 0.1 m/s for all fluids, the time elapsed from entering the channel to leaving the channel was 3.01 s at the wave height of 5 mm.

Conflict of interest

The authors declare that they have no conflict of interest in relation to this research, whether financial, personal, authorship or otherwise, that could affect the research and its results presented in this paper.

References

1. Shi, X., Tan, C., Dong, F., Murai, Y. (2019). Oil-gas-water three-phase flow characterization and velocity measurement based on time-frequency decomposition. International Journal of Multiphase Flow, 111, 219–231. doi: https://doi.org/10.1016/j.ijmultiphaseflow.2018.11.006
2. Wang, D., Jin, N., Zhai, L., Ren, Y. (2020). Characterizing flow instability in oil-gas-water three-phase flow using multi-channel conductance sensor signals. Chemical Engineering Journal, 386, 121237. doi: https://doi.org/10.1016/j.cej.2019.03.113
3. Ahmadpour, A., Noori Rahim Abadi, S. M. A. (2019). Thermal-hydraulic performance evaluation of gas-liquid multiphase flows in a vertical sinusoidal wavy channel in the presence/absence of phase change. International Journal of Heat and Mass Transfer, 138, 677–689. doi: https://doi.org/10.1016/j.ijheatmasstransfer.2019.04.084
4. Rodrigues, H., Pereyra, E., Sarica, C. (2018). Pressure Effects on Low-Liquid Loading Oil-Gas Flow in Slightly Upward Inclined Pipes: Flow Pattern, Pressure Gradient and Liquid Holdup. SPE Annual Technical Conference and Exhibition. doi: https://doi.org/10.2118/191543-ms
5. Mohmmed, A. O., Al-Kayiem, H. H., A.B., O., Sabir, O. (2020). One-way coupled fluid–structure interaction of gas–liquid slug flow in a horizontal pipe: Experiments and simulations. Journal of Fluids and Structures, 97, 103083. doi: https://doi.org/10.1016/j.jfluidstructs.2020.103083
6. Mustafa, M. A., Abdullah, A. R., Hasan, W. K., Habeeb, L. J., Nassar, M. F. (2021). Two-way fluid-structure interaction study of twisted tape insert in a circular tube having integral fins with nanofluid. Eastern-European Journal of Enterprise Technologies, 3 (8 (111)), 25–34. doi: https://doi.org/10.15587/1729-4061.2021.234125

7. Alpeissov, Y., Iskakov, R., Issenov, S., Ukenova, A. (2022). Obtaining a formula describing the interaction of fine particles with an expanding gas flow in a fluid layer. Eastern-European Journal of Enterprise Technologies, 2 (1 (116)), 87–97. doi: https://doi.org/10.15587/1729-4061.2022.255258
8. Zhang, D., Jiang, E., Zhou, J., Shen, C., He, Z., Xiao, C. (2020). Investigation on enhanced mechanism of heat transfer assisted by ultrasonic vibration. International Communications in Heat and Mass Transfer, 115, 104523. doi: https://doi.org/10.1016/j.icheatmasstransfer.2020.104523
9. Zhang, D., Zhang, H., Rui, J., Pan, Y., Liu, X., Shang, Z. (2020). Prediction model for the transition between oil–water two-phase separation and dispersed flows in horizontal and inclined pipes. Journal of Petroleum Science and Engineering, 192, 107161. doi: https://doi.org/10.1016/j.petrol.2020.107161
10. Guo, W., Wang, L., Liu, C. (2020). Thermal diffusion response to gas–liquid slug flow and its application in measurement. International Journal of Heat and Mass Transfer, 159, 120065. doi: https://doi.org/10.1016/j.ijheatmasstransfer.2020.120065
11. Pan, Y., Ji, S., Tan, D., Cao, H. (2020). Cavitation-based soft abrasive flow processing method. The International Journal of Advanced Manufacturing Technology, 109 (9-12), 2587–2602. doi: https://doi.org/10.1007/s00170-020-05836-3
12. Suleimenov, U., Zhangabay, N., Utelbayeva, A., Azmi Murad, M. A., Dosmakanbetova, A., Abshenov, K. et. al. (2022). Estimation of the strength of vertical cylindrical liquid storage tanks with dents in the wall. Eastern-European Journal of Enterprise Technologies, 1 (7 (115)), 6–20. doi: https://doi.org/10.15587/1729-4061.2022.252599